

# Liquid Phase Synthesis of MTBE from Methanol and Isobutene over Acid Zeolites and Amberlyst-15

F. Collignon, R. Loenders,\* J. A. Martens,\* P. A. Jacobs,\* and G. Poncelet<sup>1</sup>

Unité de Catalyse et Chimie des Matériaux Divisés, Université Catholique de Louvain, Place Croix du Sud 2/17, B-1348 Louvain-la-Neuve, Belgium; and \*Centrum voor Oppervlaktechemie en Katalyse, Katholieke Universiteit Leuven, Kardinaal Mercierlaan, 92, B-3001 Heverlee, Belgium

Received April 15, 1998; revised September 20, 1998; accepted November 19, 1998

The liquid phase synthesis of methyl tert-butyl ether (MTBE) from methanol and isobutene over H-Beta and US-Y zeolite catalysts was studied in the temperature range 30–120°C. Up to 100°C, commercial H-Beta zeolite samples with small crystal size were more active than acid Amberlyst-15 (reference catalyst) and noticeably more active than US-Y, confirming results obtained under vapour phase conditions. The influence of methanol/isobutene (MeOH/IB) molar ratio, pressure, and space time on the conversion and MTBE selectivity was investigated. At optimized reaction conditions, MTBE yields of 85–90% can be reached with zeolite H-Beta as well as Amberlyst-15. On zeolites, side reactions of isobutene are more important than on Amberlyst-15, necessitating operation at MeOH/IB ratios higher than 1 : 1. For the same reason, at high conversion on H-Beta, the MTBE yields are more sensitive to contact time compared to Amberlyst-15. On H-Beta zeolite, no deactivation was observed during a period of more than 50 h on stream at 65°C, 1.4 MPa pressure, and a WHSV of 14 h<sup>-1</sup>. The catalytic activity of the zeolites is related to the external specific surface area, and to the concentration of bridging hydroxyls and silanol groups in the mesopores. A zeolite H-Beta sample with a Si/Al ratio of 36 has an optimum silanol and bridging hydroxyl content leading to stoichiometric methanol and isobutene adsorption, highest activity and MTBE yields. © 1999 Academic Press

**Key Words:** MTBE; liquid phase synthesis; beta zeolites.

## INTRODUCTION

Methyl tert-butyl ether (MTBE), the most widely used octane booster for reformulated gasolines, is produced in the liquid phase over sulfonic acid resins (e.g., Amberlyst-15) at temperatures in the range 50–70°C, pressures between 1.0 and 1.5 MPa, and methanol/isobutene (MeOH/IB) molar ratios higher than 1 : 1 (1). Di-isobutenes (2,4,4 trimethyl-1- and -2-pentenenes), tert-butyl alcohol, and dimethylether are the main side products. The reaction is exothermic ( $\Delta H = -37$  kJ mol<sup>-1</sup>), and, therefore, careful control of temperature is required in order to avoid local overheating and release of sulfonic groups and sulfuric acid from

the catalyst, causing a loss of activity and giving rise to corrosion problems (2, 3). The MeOH/IB molar ratios above stoichiometry employed in order to ensure complete conversion of the isobutene necessitate a recycling operation.

The use of alternative catalysts for MTBE synthesis has been reviewed by Hutchings *et al.* (4). In recent years, many catalytic systems have been evaluated under vapour phase conditions as potential substitutes to resins, such as zirconium phosphates (5), sulfated zirconia (6, 7), titanium silicalite (8), gallophosphate cloverite (9, 10), heteropolyacids either unsupported (11, 12) or supported on silica (13), clays (14), and active carbon (15). Hydrogen zeolites, steam-dealuminated zeolites, and triflic acid-loaded zeolites have been considered as well (16–25).

In a previous study, several acidic zeolites, including H-ZSM-5, large- and small-pore H-Mordenites, H-Omega, US-Y, H-Beta, and SAPO-5, were evaluated as catalysts for the vapour phase synthesis of MTBE (26). It was found that zeolite H-Beta and acid Amberlyst-15 (Amb.-15) had similar activities, and were more active than the other zeolites tested, a result which was recently confirmed by Hunger *et al.* (27). In the present work, we extended the comparison of H-Beta and Amberlyst-15 to the liquid phase, which are the conditions applied in current industrial processes.

## EXPERIMENTAL

### Catalysts

Four samples of zeolite H-Beta and one sample of US-Y were selected for this study. Some physicochemical and textural properties of these samples are given in Table 1. The reference catalyst was Amberlyst-15 (sulfonic acid resin from Aldrich).

Zeolite US-Y (CBV 760) and zeolite H-Beta (ZB25 and ZB75) were commercial samples supplied by PQ. ZBSC, another H-Beta zeolite, was provided by Süd-Chemie. ZBF was a zeolite Beta sample synthesized according to the procedure of Caulet *et al.* (28) and having a much larger crystal size (smaller external surface area). Sample CBV 760, an ultrastable Y from PQ, was selected because it was the most

<sup>1</sup> To whom correspondence should be addressed.

TABLE 1

Crystal Size, Relative Crystallinity, Si/Al Ratio, Al Bulk, Cation Exchange Capacity (NH<sub>4</sub><sup>+</sup>-CEC), Thermodesorption of Ammonia (NH<sub>3</sub>-TPD), and Ammonia Desorption Enthalpy ( $\Delta H$ )

Sample	Crystal size ( $\mu\text{m}$ )	Rel. cryst. (%)	Si/Al <sup>a</sup>	Si/Al <sup>b</sup>	Al (mmol g <sup>-1</sup> ) <sup>b</sup>	NH <sub>4</sub> <sup>+</sup> -CEC (meq g <sup>-1</sup> )	NH <sub>3</sub> -TPD (mmol g <sup>-1</sup> )	TPD/CEC	$\Delta H$ (kJ mol <sup>-1</sup> ) <sup>c</sup>
ZB25	0.1–0.7 <sup>d</sup>	100	12.2	15.3	1.26	1.02	0.90	0.88	121
ZB75	0.1–0.7 <sup>d</sup>	96	36.0	39.8	0.45	0.41	0.41	1.00	123
ZBSC	n.d.	97	24.6	25.8	0.65	0.62	0.45	0.73	123
ZBF	1–3	72	6.7	19.5	2.17	0.81	0.41	0.51	n.d.
CBV 760	0.4–0.6 <sup>d</sup>	40	30.0	36.7	0.52	0.44	0.20	0.45	n.d.

Note. n.d., not determined.

<sup>a</sup> From ICPS analysis.

<sup>b</sup> From NH<sub>4</sub><sup>+</sup>-CEC.

<sup>c</sup> Calculated according to Ref. (31).

<sup>d</sup> Data from PQ.

active sample among a series of US-Y zeolites tested under vapour phase conditions (26).

### Characterization

The relative crystallinity of the H-Beta zeolites (Table 1) was evaluated from the X-ray diffraction patterns recorded with a Siemens D-5000 diffractometer (with copper anticathode), referring the area of the [302] reflection at 22.43° 2 $\theta$  to that of sample ZB25. For CBV 760, the crystallinity was related to that of the parent CBV 500 (26). The Si/Al ratios determined from the elemental analyses performed by ICPS are indicated in Table 1. The X-ray diffraction pattern of ZBF showed the presence of a small amount of pseudo-boehmite (with interplanar distances of 0.615, 0.317, and 0.240 nm), and, therefore, the Si/Al ratio of 6.7 of this sample derived from the bulk analysis is underestimated.

The textural characteristics were derived from the nitrogen adsorption isotherms recorded at the boiling point of nitrogen with an ASAP 2000 sorptometer from Micromeritics, after outgassing the samples for 4 h at 200°C. The external surface areas and micropore volumes,  $S_{\text{ext}}$  and  $V_{\mu}$ , respectively, were established using an approach recently proposed (29). The mesopore distributions were calculated using the Barrett–Joyner–Halenda method based on Kelvin equation (30). The experimental values are given in Table 2. The pore size distribution in the meso- and macropore region of the different zeolites was examined. As seen in Fig. 1, distinct distribution curves are observed: ZB25, ZB75, and ZBSC have pores in the mesopore range 20–500 Å. ZBF, with the smallest external surface area among the Beta zeolites and the largest particles, is almost exempt of mesopores (0.04 cm<sup>3</sup> g<sup>-1</sup>). The data for the US-Y zeolites were added for comparison. US-Y CBV 760 has fewer mesopores ( $V_{\text{meso}} = 0.19 \text{ cm}^3 \text{ g}^{-1}$ ).

The cation exchange capacity (NH<sub>4</sub><sup>+</sup>-CEC) of the samples was determined by the micro-Kjeldahl method on ammonium-exchanged samples. The ammonium form of

the zeolites was obtained by treating typically 1 g of zeolite overnight at 80°C under reflux conditions with 200 ml of 2 M ammonium acetate solution. The slurry was filtered hot, washed with demineralized water until the conductivity of the wash water was reduced to its initial value, and dried at 60°C for 1 h. Using these NH<sub>4</sub><sup>+</sup>-CEC values, the Si/Al ratios were recalculated (Si/Al<sup>c</sup> in Table 1), assuming that each exchanged NH<sub>4</sub><sup>+</sup> cation site is associated with one tetrahedral (framework) Al.

Temperature-programmed desorption of ammonia (NH<sub>3</sub>-TPD) was carried out following the experimental conditions proposed by Niwa *et al.* (31) and Katada *et al.* (32), which allow one to determine the desorption enthalpies of ammonia from the high-temperature desorptions and, hence, to provide an evaluation of the average acid strength of the zeolites. TPD was monitored with a TC detector and the ammonia in the gaseous effluent at the outlet of the detector continuously trapped in 0.2 M H<sub>3</sub>BO<sub>3</sub> solution. The total amount of ammonia evolved was determined by

TABLE 2

External Surface Area ( $S_{\text{ext}}$ ), Micropore Volume ( $V_{\mu}$ ), Total Pore Volume ( $V_{\text{tot}}$ ), Mesoporous Volume ( $V_{\text{meso}}$ ), and Relative Silanol Concentration ([SiOH])

Sample	$S_{\text{ext}}$ (m <sup>2</sup> g <sup>-1</sup> ) <sup>a</sup>	$V_{\mu}$ (cm <sup>3</sup> g <sup>-1</sup> ) <sup>a</sup>	$V_{\text{tot}}$ (cm <sup>3</sup> g <sup>-1</sup> ) <sup>b</sup>	$V_{\text{meso}}$ (cm <sup>3</sup> g <sup>-1</sup> ) <sup>c</sup>	[SiOH] (a.u. g <sup>-1</sup> ) <sup>d</sup>
ZB25	219	0.23	1.22	0.52	100
ZB75	218	0.21	1.17	0.49	143
ZBSC	124	0.21	1.08	0.18	110
ZBF	30	0.17	0.24	0.04	n.d.
CBV 760	143	0.25	0.47	0.16	n.d.

Note. n.d., not determined.

<sup>a</sup> Calculated according to Ref. (29).

<sup>b</sup> Calculated with N<sub>2</sub> sorption at  $p/p_0 = 0.99$ .

<sup>c</sup> Calculated according to Ref. (30).

<sup>d</sup> From FTIR (normalized integrated area of the band at 3740 cm<sup>-1</sup>).

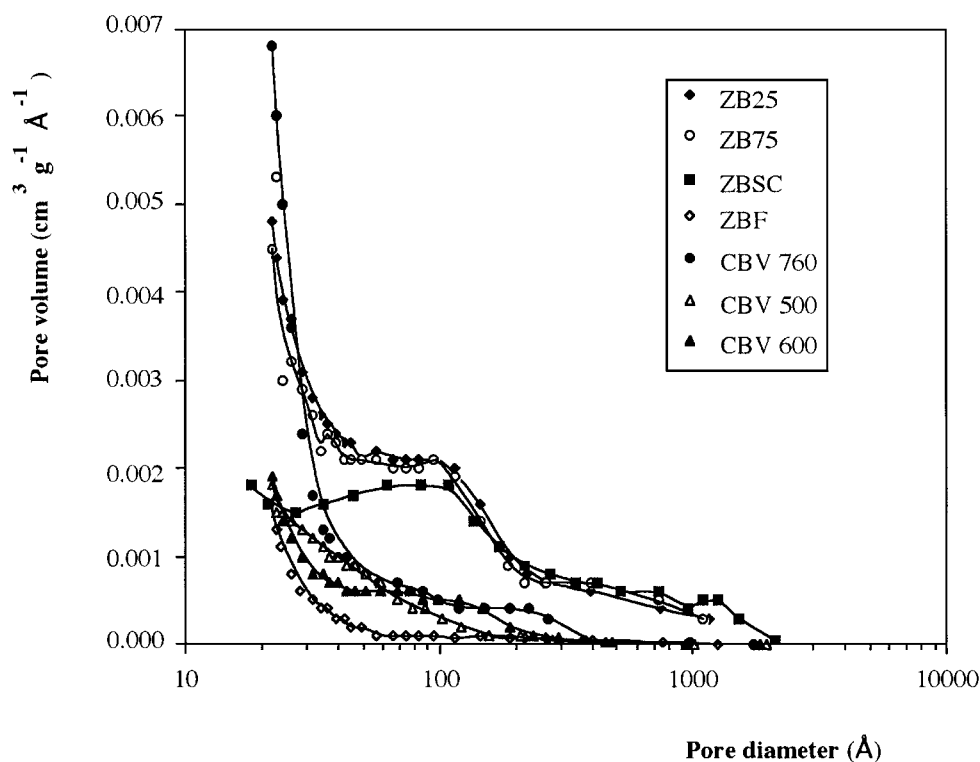


FIG. 1. Pore size distribution curves of H-Beta zeolites (ZB25, ZB75, ZBF, and ZBSC) and US-Y zeolites (CBV 500, CBV 600, and CBV 760).

backtitration with 0.005 M  $\text{H}_2\text{SO}_4$ . The desorption enthalpies are indicated in Table 1.

Infrared spectra were recorded with a Bruker FTIR IFS-88 spectrometer on wafers obtained by compression ( $15 \text{ mg cm}^{-2}$ ). In this study, only the OH stretching region will be considered. The samples were outgassed at  $400^\circ\text{C}$  for 4 h under a residual pressure of  $10^{-3} \text{ Pa}$ . The relative integrated areas of the Si-OH band at  $3740 \text{ cm}^{-1}$  normalized to the sample weight are indicated in Table 2.

The adsorption capacities of MeOH and IB of the zeolites and Amberlyst-15 were evaluated under precatalytic dynamic conditions in the installation used for the vapour phase synthesis of MTBE (26) and equipped with on-line gas chromatographic analysis. The conditions were as follows: weight of catalyst = 200 mg; MeOH : IB : He = 1 : 1 : 5;  $P = 0.1 \text{ MPa}$ ; WHSV =  $3.25 \text{ h}^{-1}$ ; temperature =  $27^\circ\text{C}$ . The amounts of isobutene and methanol retained by the different zeolites and the resin determined from the breakthrough curves of the two compounds are indicated in Table 3. The saturation capacities are accurate within 5%.

#### Catalytic Experiments

The reactions were carried out in the liquid phase in a fixed bed stainless-steel reactor operated, unless otherwise specified, at 2 MPa, using a MeOH : IB molar ratio of 1, and a WHSV of  $14 \text{ h}^{-1}$ . Methanol was blended with isobutene in a pressure vessel, and the stirred mixture was injected

in the reactor via a mass flow controller for liquids (from Brooks Instrument B.V.). Pressurisation was ensured by nitrogen. The reaction was studied in the temperature range  $30\text{--}120^\circ\text{C}$ . A thermocouple placed in the catalyst bed (1 g) allowed continuous monitoring of the reaction temperature. All tubings, valves, and connections between the outlet of the reactor and the gas chromatograph were heated.

On-line analysis of the reaction products was done in a HP-5890 gas chromatograph (from Hewlett-Packard) equipped with flame ionization detector and 50 m capillary column (CPSil-5-CB, film thickness:  $5.49 \mu\text{m}$ ). Sampling of the liquid effluent was done every hour by means of an automated six-way sampling valve with internal volume of  $0.1 \mu\text{l}$  (Valco Instrument Co.). The temperature of the

TABLE 3

Amounts of Adsorbed Methanol and Isobutene ( $\text{mmol g}^{-1}$ ) and Molar Ratios

Catalyst	Methanol (MeOH)	Isobutene (IB)	MeOH/IB
Amb.-15	7.48	2.64	2.83
ZB25	4.50	3.08	1.46
ZB75	4.83	4.58	1.05
ZBSC	3.78	2.54	1.49
ZBF	1.64	1.24	1.32
CBV 760	6.93	4.80	1.44

reactor was increased by 10°C after each sampling of the reaction products. Prior to the catalytic evaluation, the zeolite was activated *in situ* at 400°C for 3 h under a stream of nitrogen. The reference Amberlyst-15 was first washed (water and alcohol) using the procedure of Volosch *et al.* (33) and pretreated *in situ* at 90°C for 3 h in flowing nitrogen.

## RESULTS

### Screening Tests and Influence of Temperature on the Catalytic Activity

For the different zeolites and the acid resin (Amb.-15) catalysts, the variations of the conversion of isobutene (IB) and of the isobutene based yield of MTBE with reaction temperature are compared in Figs. 2a and 2b, respectively. The IB conversions (Fig. 2a) increased with increasing reaction temperature to reach a maximum of 95% at around 100°C for ZB25, ZB75, and ZBSC, and of about 92–93% for Amb.-15. These H-Beta zeolites were more active than Amb.-15. The ZB75 catalyst was most active in terms of IB conversion, with an isobutene conversion above 90% at 60°C. ZBF and, especially, US-Y were less active, with conversions of 85 and 75%, respectively, at 100°C.

On Amb.-15, ZBF, and US-Y, the IB-based yield of MTBE (Fig. 2b) increased continuously with reaction temperature. On the more active ZB25, ZB75, and ZBSC, the MTBE yield passed through a maximum at around 60, 70, and 75°C, respectively. The decreasing yields of MTBE noticed above 60–80°C for ZB25, ZB75, and ZBSC are due to a loss of MTBE selectivity because of increasing dimerisation of isobutene.

According to the thermodynamics of the reaction, at 65°C and 1.6 MPa, and for a MeOH:IB ratio of 1:1, the MTBE yield at equilibrium amounts to 91.5% (34). In our experiments, with none of the zeolites the thermodynamic equilibrium represented in Fig. 2b was reached. The conversion of IB, the yield of MTBE, and the selectivities observed at 50, 65, and 90°C are detailed in Table 4. Except

for ZBSC at 65°C, the H-Beta zeolites were less selective than the resin. US-Y was very selective at low conversions.

### Influence of Pressure

The influence of pressure (0.6, 1, 1.4, and 2 MPa) was examined for the zeolite ZB75 and the resin, with a MeOH:IB ratio of 1 and WHSV of 14 h<sup>-1</sup>. For both catalysts, pressure only had a limited influence on the conversion of isobutene, as expected under liquid phase conditions. In the case of the zeolite, beyond the maximum conversion of IB to MTBE, the undesired oligomerisation of IB was relatively more enhanced at high pressure. A similar observation was reported by Obenaus and Droste (35).

### Influence of MeOH:IB Molar Ratio

Experiments were performed on ZB75 and Amberlyst-15 with three MeOH:IB ratios, 1, 1.2, and 1.5, at a pressure of 2.0 MPa and WHSV of 14 h<sup>-1</sup>. The variations of the conversion of IB and of the yield of MTBE with temperature are shown in Figs. 3a and 3b, and 4a and 4b for ZB75 and the resin, respectively. On the zeolite, in the temperature range of increasing conversions, similar conversion curves are obtained for MeOH/IB ratios of 1 and 1.2 (up to about 70°C, Fig. 3a) but higher maximum yields to MTBE are reached for the ratio 1.2 compared to 1 (Fig. 3b). For the ratio 1.5, the IB conversion curve is shifted to higher temperatures and nearly similar IB conversions are achieved above 80°C. However, at 70°C and above, the MTBE yield is improved with respect to the lower MeOH/IB ratios (Fig. 3b). On the resin, the IB conversion increases with increasing MeOH/IB ratio (Fig. 4a). The yields of MTBE improve when increasing this ratio (Fig. 4b). The maximum yields of MTBE are less influenced by the MeOH/IB ratio, but the maximum value is reached at lower temperatures as the MeOH/IB ratio increases.

The catalytic results obtained at 60 and 90°C (2 MPa, WHSV of 14 h<sup>-1</sup>) on H-Beta ZB75 and on the resin for the different MeOH/IB ratios are compared in Table 5. For

TABLE 4

Isobutene Conversion ( $X_{IB}$ ); Yield IB to MTBE ( $Y_{MTBE}$ ); Selectivity to MTBE ( $S_{MTBE}$ ) at 50, 65, and 90°C; and Apparent MTBE Formation Rate at 50°C (mol h<sup>-1</sup> g<sup>-1</sup>)

Catalyst	T (°C):	$X_{IB}$ (%)			$Y_{MTBE}$ (%) <sup>a</sup>			$S_{MTBE}$ (%)			Rate 50
		50	65	90	50	65	90	50	65	90	
Amb.-15		26	72	90	25	68	87	98	94	97	0.039
ZB25		52	85	95	49	76	65	93	89	68	0.077
ZB75		68	94	96	62	82	65	92	87	68	0.099
ZBSC		33	85	95	32	81	83	97	95	87	0.051
ZBF		7	30	82	7	28	74	97	93	90	0.011
CBV 760		3	7	71	3	7	63	100	100	89	0.005

Note. Reaction conditions:  $P = 2.0$  MPa; MeOH/IB = 1; WHSV = 14 h<sup>-1</sup>.

<sup>a</sup> For the yields at equilibrium, multiply the values at 50, 65, and 90°C by 1.03, 1.04, and 1.07, respectively.

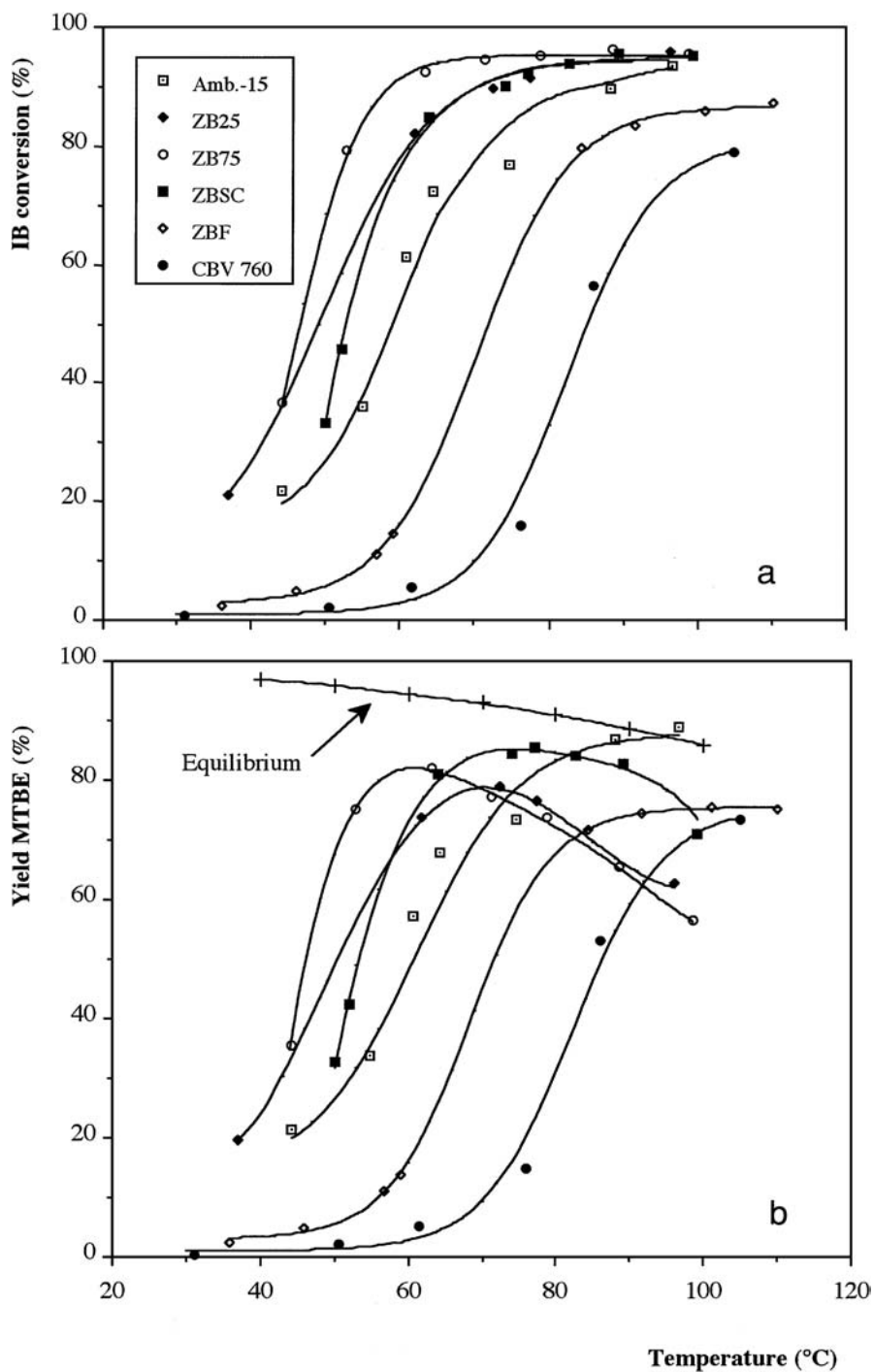


FIG. 2. Isobutene conversion (a) and IB to MTBE yields (b) vs reaction temperature on Amberlyst-15, H-Beta zeolites (ZB25, ZB75, ZBF, and ZBSC), and US-Y (CBV 760). Reaction conditions:  $P = 2$  MPa; MeOH/IB = 1; WHSV =  $14 \text{ h}^{-1}$ .

both catalysts, higher conversions of isobutene are achieved at  $90^\circ\text{C}$  than at  $60^\circ\text{C}$ . The influence of the MeOH/IB ratio on the conversion is more marked for the resin than for the zeolite. The temperature dependence of the selectivity of isobutene to MTBE is more pronounced for the zeolite compared with the resin and, as expected, the methanol conversion decreases as the MeOH/IB ratio increases.

#### *Influence of WHSV*

Results of experiments performed at different WHSV over ZB75 (MeOH:IB ratio of 1; 2 MPa pressure;  $60^\circ\text{C}$ ) are presented in Table 6. Increasing WHSV had a beneficial effect on the yields of MTBE and on the selectivity, whereas the total conversion of IB decreased. These

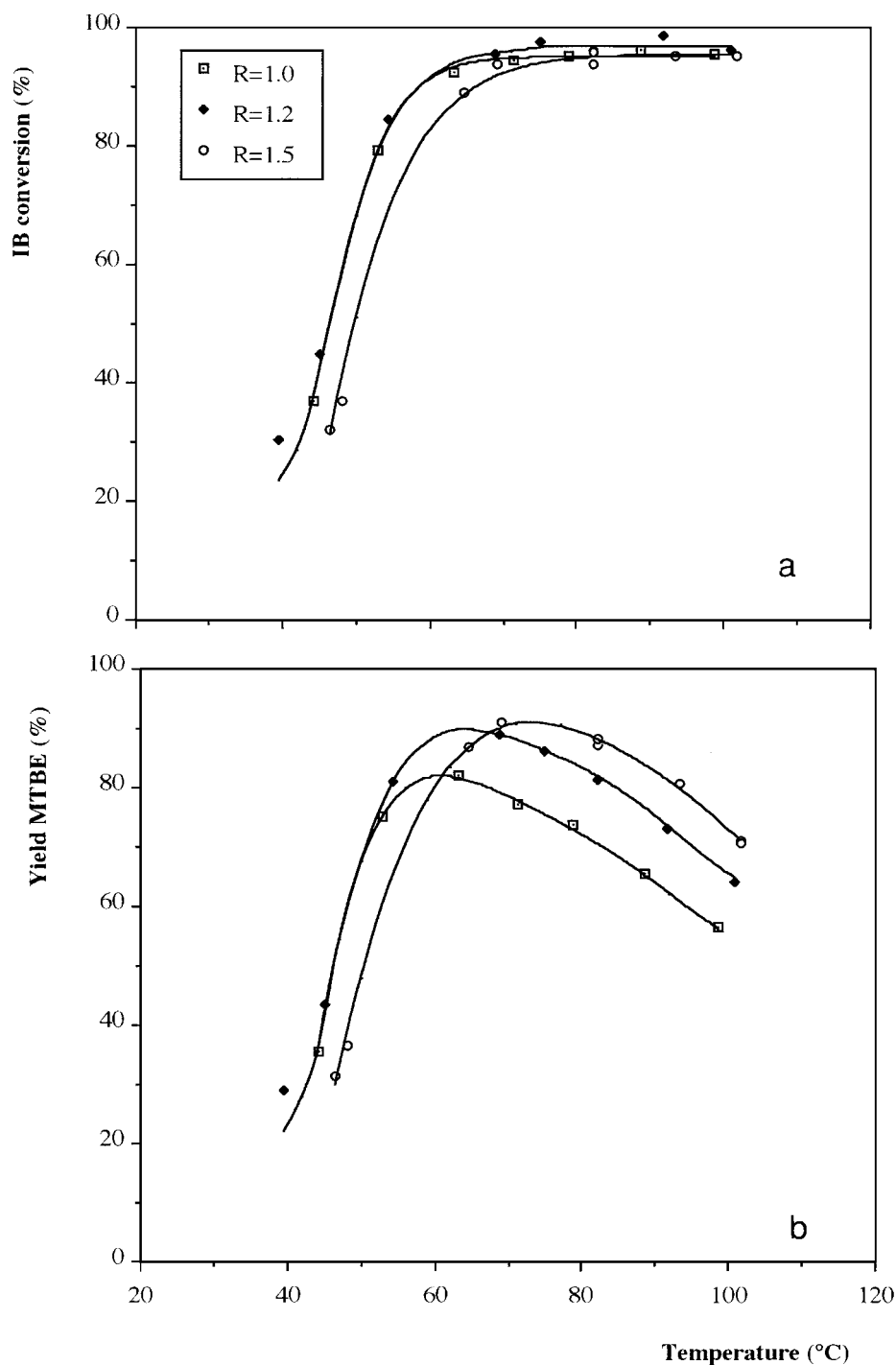


FIG. 3. Influence of MeOH/IB molar ratio: isobutene conversion (a) and IB to MTBE yield (b) vs temperature on ZB75. Reaction conditions:  $P=2$  MPa;  $WHSV=14$  h<sup>-1</sup>.

data show that long contact times with the zeolite catalyst at high conversion should be avoided. This could be explained by lower methanol concentration in the reactant stream, making dimerisation more likely. Alternatively, the losses of MTBE yield at long contact times could be due to a secondary conversion of the MTBE into methanol and

isobutene oligomers. This effect should be attenuated at higher MeOH/IB ratios, as may be inferred from Fig. 3.

#### Durability Test

A prolonged test was performed at 65°C on ZB75, under the following conditions: pressure of 1.4 MPa, WHSV of

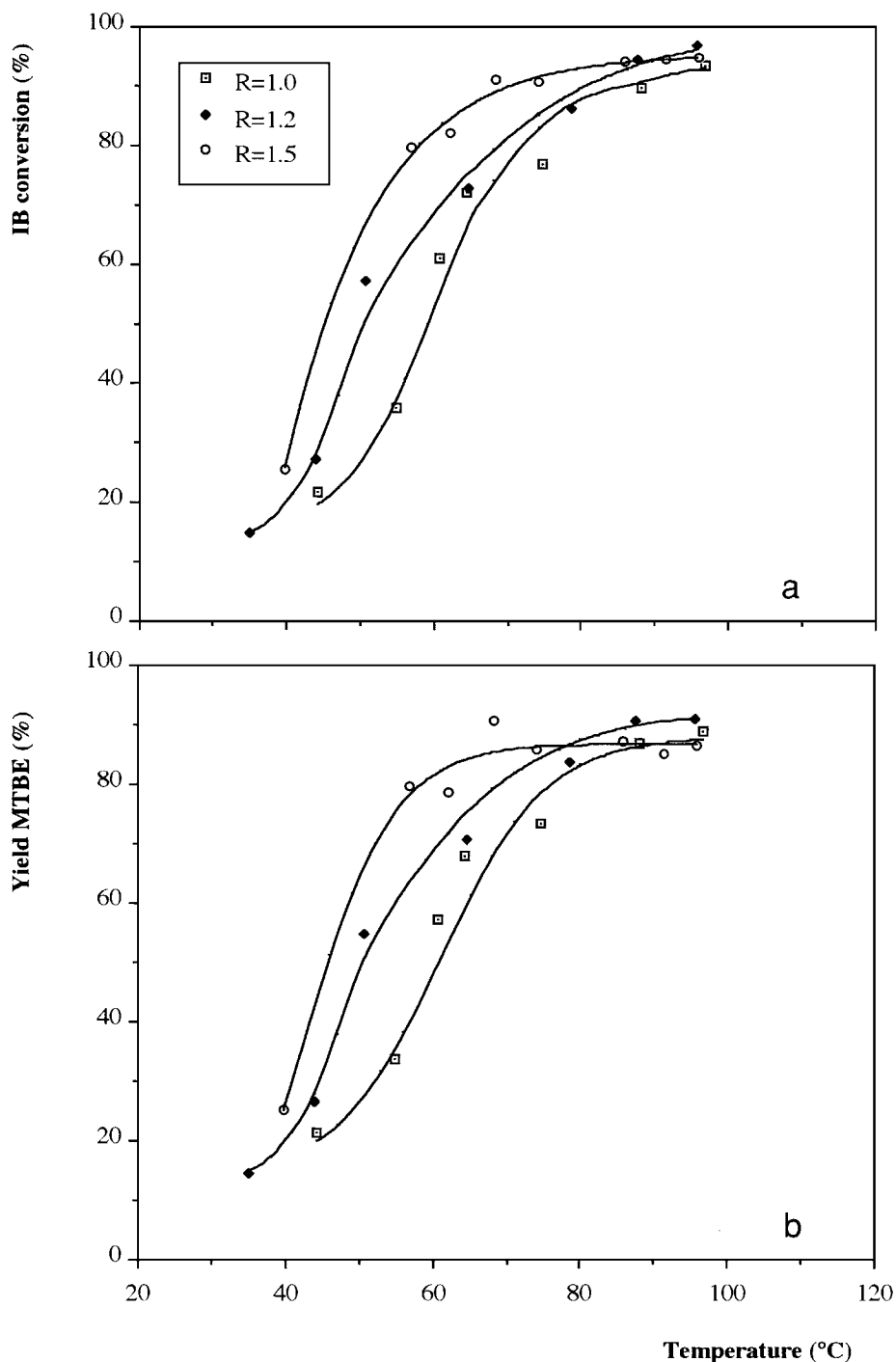


FIG. 4. Influence of MeOH/IB molar ratio: isobutene conversion (a) and IB to MTBE yield (b) vs temperature on Amberlyst-15. Reaction conditions: same as in Fig. 2.

$14 \text{ h}^{-1}$ , and MeOH:IB of 1. As shown in Fig. 5, the conversion of IB remained stable during 53 h on stream. The transformation of IB to MTBE stabilised at a value of 82% with a selectivity of 87%. No tert-butyl alcohol was formed and the yields of oligomerisation products remained constant. Under these experimental conditions, a total weight

of MTBE of 638 g per g catalyst was produced without noticeable loss of activity. The resin operating under industrial conditions has a lifetime of at most 2 years. Considering a feed containing 20–30% C<sub>4</sub>, with half of it being isobutene, a rough estimate of the production of MTBE would amount to 4000 g MTBE per g resin assuming  $16 \times 10^3 \text{ h}$  lifetime of

TABLE 5

Isobutene and Methanol Conversion ( $X_{IB}$ ;  $X_{MeOH}$ ), Yield of MTBE ( $Y_{MTBE}$ ), and Selectivity ( $S_{IB,MTBE}$ ;  $S_{MeOH,MTBE}$ ) on ZB75 and Amb.-15 for Different MeOH/IB Molar Ratios at 60 and 90°C

Catalyst	$T$ (°C)	MeOH/IB	$X_{IB}$ (%)	$Y_{MTBE}^a$ (%)	$S_{IB,MTBE}$ (%)	$X_{MeOH}$ (%)	$S_{MeOH,MTBE}$ (%)
ZB75	60	1.0	90	82	91	82	100
		1.2	90	87	97	72	100
		1.5	88	75	85	50	100
	90	1.0	95	64	67	66	100
		1.2	97	74	76	62	100
		1.5	95	83	87	51	100
Amb.-15	60	1.0	60	55	92	62	100
		1.2	70	67	96	54	100
		1.5	80	79	99	53	100
	90	1.0	90	87	97	89	100
		1.2	94	90	96	78	100
		1.5	94	87	93	51	100

Note. Reaction conditions:  $P = 2.0$  MPa;  $WHSV = 14$  h<sup>-1</sup>.

<sup>a</sup> For the yields at equilibrium, multiply the values at 60 and 90°C by 1.04 and 1.07, respectively.

the resin and  $WHSV$  of 1 h<sup>-1</sup>. Of course, in the laboratory a prolonged activity test could not be envisaged. However, the present data suggest that a productivity figure similar to the one obtained on the resin might be within reach with a H-Beta zeolite.

TABLE 6

Isobutene Conversion ( $X_{IB}$ ), Yield of MTBE ( $Y_{MTBE}$ ), and Selectivity to MTBE ( $S_{MTBE}$ ) on ZB75 for Different  $WHSV$  at 60°C

$WHSV$ (h <sup>-1</sup> )	$X_{IB}$ (%)	$Y_{MTBE}$ (%) <sup>a</sup>	$S_{MTBE}$ (%)
9	95	77	81
14	92	82	89
28	90	83	92

Note. Reaction conditions:  $P = 2.0$  MPa; MeOH/IB = 1.

<sup>a</sup> For the yields at equilibrium, multiply the values by 1.04.

## DISCUSSION

The activity sequence of the H-Beta and US-Y zeolites tested in the liquid phase synthesis of MTBE is similar to that found under vapour phase conditions, where the resin and ZB25 and ZB75 samples reached MTBE yields of 50–51% (26), significantly higher than for US-Y (29%), the next most active zeolite. In the vapour phase synthesis, a correlation was found between the maximum yield of MTBE and the external surface area of the zeolite (26). In the liquid phase synthesis, it is now also found that the apparent MTBE formation rate at 50°C is proportional to the external surface area of the zeolite (Fig. 6). ZB75 and ZB25 having the highest external surface area are the most active samples. It may be inferred from this dependence

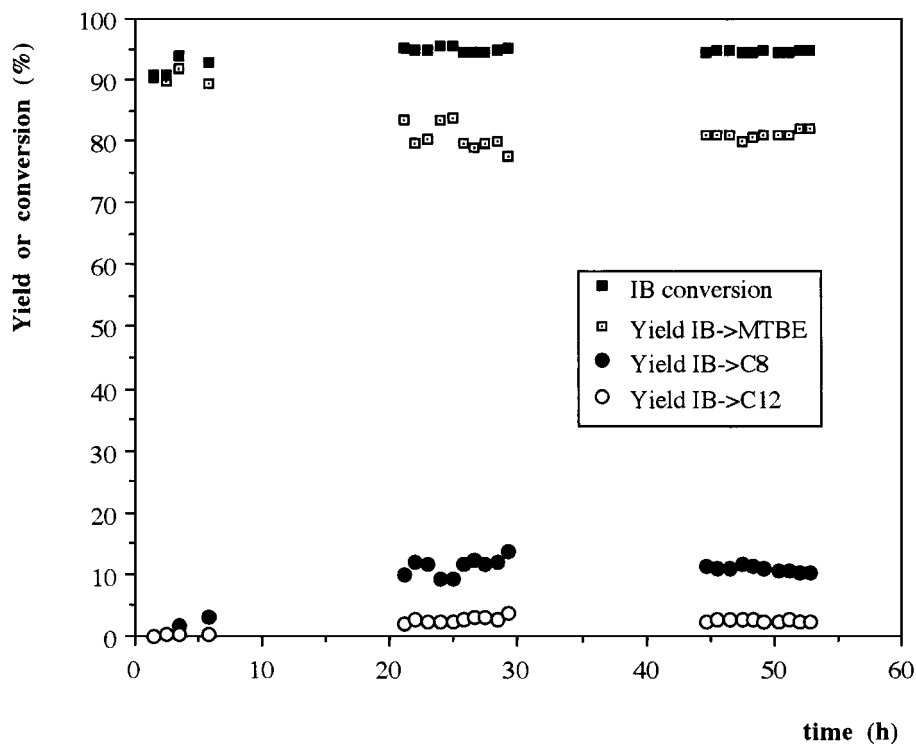


FIG. 5. Isobutene conversion, yield of IB to MTBE, and of the by-products vs time on stream on ZB75. Reaction conditions:  $P = 1.4$  MPa,  $WHSV = 14$  h<sup>-1</sup>; MeOH/IB = 1;  $T = 65^\circ\text{C}$ .



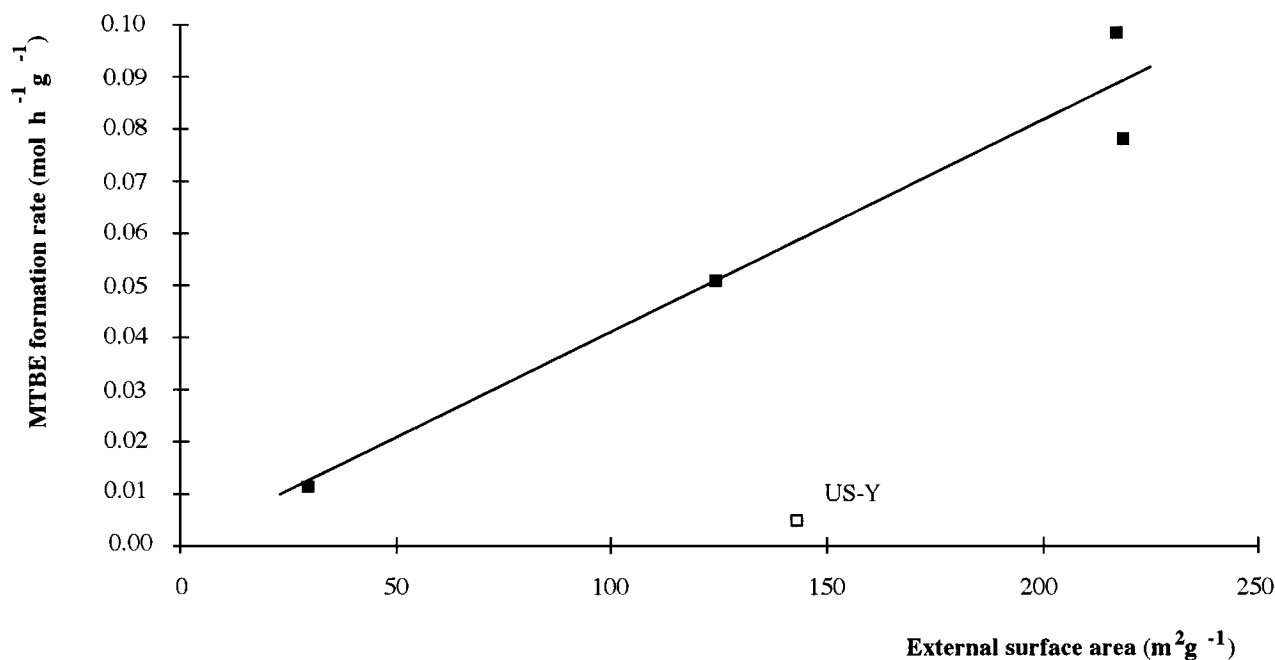


FIG. 6. Variation of MTBE formation rate at 50°C (in  $\text{mol g}^{-1} \text{h}^{-1}$ ) vs external surface area ( $S_{\text{ext}}$ , in  $\text{m}^2 \text{g}^{-1}$ ) of H-Beta zeolites (ZB25, ZB75, and ZBSC) (full symbols), and US-Y (CBV 760) (open symbol).

that the reaction is strongly diffusion limited and that only the active sites near the external surface contribute to the catalytic turnovers, while the bulk of the zeolite crystals is inactive. A similar situation was encountered in the liquid phase alkylation of isobutane with 1-butene (36) and phenol alkylation with tert-butyl alcohol (37), both on Beta zeolite. The difference in activity of ZB25 and ZB75 (Fig. 6), having the same external surface area of ca.  $220 \text{ m}^2 \text{g}^{-1}$  (Table 1), remains to be explained.

Dealuminated zeolites have been shown to be more active than their nondealuminated forms in a large number of proton-catalyzed reactions (19–23). A similar observation was made in the vapour phase synthesis of MTBE (26). It is not known whether ZB75 is a dealuminated form of ZB25 or the result of direct synthesis, but its higher content of silanol groups (Table 1), absence of extraframework Al (inferred from the  $\text{NH}_3\text{-TPD}/\text{NH}_4^+\text{-CEC}$  ratio of 1), lower crystallinity compared with ZB25 (Table 1), and similar texture (Fig. 1, Table 1) suggest an acid dealuminated form.

The desorption enthalpies of ammonia given in Table 1 indicate that the acid sites have nearly equivalent average strengths. For ZB25 from the same source, Katada *et al.* (32) reported a  $\Delta H$  of  $122 \text{ kJ mol}^{-1}$ . Thus, based on the ammonia desorption enthalpies, differences in acid strengths can hardly be invoked to account for activity differences of ZB75 and ZB25. Moreover, the most active ZB75 has a higher Si/Al ratio and contains a lower number of acid sites.

For US-Y zeolites, extraframework aluminum (with  $^{27}\text{Al}$  NMR signal at 30 ppm) had a negative influence on the reaction rate in the vapour phase synthesis of MTBE (26). Kiricsi *et al.* (38) did not find such species in acid-dealuminated H-Beta zeolite. For the present H-Beta zeolites, the presence of extraframework aluminum can be estimated from the  $\text{NH}_3\text{-TPD}/\text{NH}_4^+\text{-CEC}$  ratios (Table 1). The ratio of 1 obtained for ZB75 indicates, within the precision of the measurements, the absence of a significant amount of extraframework Al species. In sample ZB25, the ratio is equal to 0.88, which points to the presence of some extraframework aluminum. Since this aluminum is mostly located inside the micropores, and the catalytic activity is not located in this type of pores, it seems unlikely that these species play a significant role in this catalyst.

The methanol and isobutene adsorption capacities under precatalytic conditions (Table 3) shed more light on the activity difference of ZB25 and ZB75. The saturation capacity for isobutene is significantly larger for ZB75 (4.6 compared to  $3.1 \text{ mmol g}^{-1}$ ). Dealumination of a zeolite enhances its hydrophobic character and can explain the enhanced adsorption of isobutene in ZB75. On the other hand, the adsorption capacity for methanol is very similar in these two zeolites (4.8 and  $4.5 \text{ mmol g}^{-1}$ ).

In a recent study by *in situ* H-MAS NMR spectroscopy of methanol sorption on H-Beta (with Si/Al = 16), H-ZSM-5 (Si/Al = 22), and H-Y (Si/Al = 2.6) zeolites, Hunger *et al.* (27) and Hunger and Horvath (39) showed that the preferential adsorption sites in H-ZSM-5 and H-Y are the

bridging hydroxyls (SiOHAl), whereas in H-Beta, in addition, surface silanols also contribute to the adsorption of the alcohol. Following those authors, H-Beta contains eight times more silanols per gram zeolite than the other two zeolites, and larger adsorbate complexes are formed in H-Beta than in H-ZSM-5 and H-Y. The high hydroxyl concentration in Beta zeolites has been related to the high degree of structural disorder (40–42). Moreover, Hunger and Horvath (39) observed that the methanol molecules are less tightly bonded on silanols than on bridging OH, 70% of the methanol molecules involved in the adsorbed complexes being weakly hydrogen-bonded at silanol groups. The intervention of the silanol groups was recently confirmed by *in situ* MAS-NMR spectroscopy of MTBE synthesis under continuous flow conditions (43).

The ZB75 sample contains ca. 40% more silanol groups than ZB25 (Table 1) and the share of methanol adsorbed on these weak adsorption sites must be larger in ZB75 than in ZB25. It seems that zeolite ZB75 offers an optimum combination of methanol and isobutene adsorption sites. Ultra-stable Y zeolites contain much less mesopores and silanol groups. Their much lower activity compared to zeolite Beta samples may be related to these different properties.

### CONCLUSIONS

Zeolite H-Beta samples with Si/Al ratios of 12.2 and 36 and a small crystal size exhibit a higher activity than Amberlyst-15 at temperatures between 40 and 100°C and similar MTBE selectivity up to about 90% conversion of isobutene. At high conversion, the acid resin is slightly more selective than the H-Beta zeolites, because the side reaction of oligomerization of isobutene is more pronounced in H-Beta. On H-Beta, the activity decreases with increasing MeOH/IB ratio, while the opposite is true on Amb.-15. On both types of catalysts, the MTBE selectivity increases with increasing MeOH/IB ratio. On H-Beta zeolite, MTBE seems to be converted in a secondary reaction into isobutene oligomers and methanol. This undesirable secondary reaction can be counteracted by increasing the MeOH/IB ratio or by increasing WHSV. The activity of H-Beta zeolites is proportional to their specific external surface area. The most active and selective H-Beta (ZB75) sample adsorbs isobutene and methanol in stoichiometric amounts. This sample, with Si/Al = 36 and external surface area of 218 m<sup>2</sup> g<sup>-1</sup>, contains a higher concentration of silanol groups exposed in the mesopores and does not contain extraframework Al.

### ACKNOWLEDGMENTS

F.C. is indebted to F.R.I.A. (Belgium) for a doctoral grant. J.A.M. and P.A.J. acknowledge the Belgian and Flemish governments for research grants within the frame of I.U.A.P. and G.O.A., respectively.

### REFERENCES

- Lee, A. K. K., and Al-Jarallah, A., *Chem. Econ. Eng. Rev.* **18**, 25 (1986).
- Takezono, T., and Fujiwara, Y., U.S. Patent 4,182,913 (1980).
- Vincencio, G. T., Ramos, A. O., Villanueva, J. R., and Lopez, G. P., *Rev. Inst. Mexicano Petrol.* **14**, 66 (1987).
- Hutchings, G. J., Nicolaides, C. P., and Scurrall, M. S., *Catal. Today* **15**, 23 (1992).
- Cheng, S., Wang, J.-T., and Lin, C.-L., *J. Chin. Chem. Soc.* **38**, 529 (1991).
- Feeley, O. C., Johansson, M. A., Herman, R. G., and Klier, K., *Prep. Pap. Am. Chem. Soc. Div. Fuel Chem.* **37**, 1817 (1992).
- Quiroga, M. E., Figoli, N. S., and Sedran, U. A., *Chem. Eng. J.* **67**, 199 (1997).
- Chang, K.-H., Kim, G.-J., and Ahn, W.-S., *Ind. Eng. Chem. Res.* **31**, 125 (1992).
- Richter, M., Zubowa, H.-L., Eckelt, R., and Fricke, R., *Microporous Mater.* **7**, 119 (1996).
- Richter, M., Fischer, H., Bartoszek, M., Zubowa, H.-L., and Fricke, R., *Microporous Mater.* **8**, 69 (1997).
- Shikata, S., Okuhara, T., and Misono, M., *J. Mol. Catal. A* **100**, 49 (1995).
- Baronetti, G., Briand, L., Sedran, U., and Thomas, H., *Appl. Catal. A* **172**, 265 (1998).
- Shikata, S., Nakata, S.-I., Okuhara, T., and Misono, M., *J. Catal.* **166**, 263 (1997).
- Yadav, G. D., and Kirthivasan, N., *J. Chem. Soc. Chem. Commun.*, 203 (1995).
- Chu, W. L., Yang, X. G., Ye, X. K., and Wu, Y., *React. Kinet. Catal. Lett.* **62**, 333 (1997).
- Chu, P., and Kühl, G. H., *Ind. Eng. Chem. Res.* **26**, 365 (1987).
- Pien, S. I., and Hatcher, W. J., *Chem. Eng. Comm.* **93**, 257 (1990).
- Le Van Mao, R., Carli, R., Ahlafi, H., and Ragaini, V., *Catal. Lett.* **6**, 321 (1990).
- Nikolopoulos, A. A., Oukaci, R., Goodwin, J. G., Jr., and Marcelin, G., *Prep. Pap. Am. Chem. Soc. Div. Petrol. Chem.* **37**, 787 (1992).
- Nikolopoulos, A. A., Kogelbauer, A., Goodwin, J. G., Jr., and Marcelin, G., *Appl. Catal. A* **119**, 69 (1994).
- Kogelbauer, A., Nikolopoulos, A. A., Goodwin, J. G., Jr., and Marcelin, G., *J. Catal.* **152**, 122 (1995).
- Kogelbauer, A., Nikolopoulos, A. A., Goodwin, J. G., Jr., and Marcelin, G., in "Studies in Surface Science and Catalysis," Vol. 84, p. 1685. Elsevier, Amsterdam, 1994.
- Nikolopoulos, A. A., Kogelbauer, A., Goodwin, J. G., Jr., and Marcelin, G., *J. Catal.* **158**, 76 (1996).
- Ahmed, S. M., El-Faer, M. Z., Abdillahi, M. M., Shirokoff, J., Siddiqui, M. A. B., and Barri, S. A. I., *Appl. Catal. A* **161**, 47 (1997).
- Quiroga, M. E., Figoli, N. S., and Sedran, U. A., *React. Kinet. Catal. Lett.* **63**, 75 (1998).
- Collignon, F., Mariani, M., Moreno, S., Remy, M., and Poncelet, G., *J. Catal.* **166**, 53 (1997).
- Hunger, M., Horvath, T., and Weitkamp, J., in "Proceedings, DGMC Conference 'C4 Chemistry—Manufacture and Uses of C4 Hydrocarbons,'" p. 65. Ger. Soc. Petrol. Coal Sci. Techn., 1997.
- Caullet, P., Hazm, J., Guth, J. L., Joly, J. F., and Raatz, F., *Zeolites* **12**, 240 (1992).
- Remy, M. J., and Poncelet, G., *J. Phys. Chem.* **99**, 773 (1995).
- Barrett, E. P., Joyner, L. G., and Halenda, P. P., *J. Am. Chem. Soc.* **73**, 373 (1951).
- Niwa, M., Katada, N., Sawa, M., and Murakami, Y., *J. Phys. Chem.* **99**, 8812 (1995).
- Katada, N., Iijima, S., Igi, H., and Niwa, M., in "Studies in Surface Science and Catalysis," Vol. 105, p. 1227. Elsevier, Amsterdam, 1997.
- Volosch, M., Ladisch, M. R., and Tsao, G. T., *React. Polymers* **4**, 9 (1986).

34. Izquierdo, J. F., Cunill, F., Viña, M., Tejero, J., and Iborra, M., *J. Chem. Eng. Data* **37**, 339 (1992).
35. Obenaus, F., and Droste, W., *Oil Gas J.* **77**, 76 (1979).
36. Loenders, R., Jacobs, P. A., and Martens, J. A., *J. Catal.* **176**, 545 (1998).
37. Zhang, K., Huang, C., Zhang, H., Xiang, S., Liu, S., Xu, D., and Li, H., *Appl. Catal. A* **166**, 89 (1998).
38. Kiricsi, I., Flego, C., Pazzuconi, G., Parker, Jr., W. O., Millini, R., Perego, C., and Bellussi, G., *J. Phys. Chem.* **98**, 4627 (1994).
39. Hunger, M., and Horvath, T., *Catal. Lett.* **49**, 95 (1997).
40. Treacy, M. M. J., and Newsam, J. M., *Nature* **332**, 249 (1988).
41. Newsam, J. M., Treacy, M. M. J., Koetsier, W. J., and de Gruyter, C. B., *Proc. R. Soc. London A* **420**, 375 (1988).
42. Pazé, C., Bordiga, S., Lamberti, C., Salvalaggio, M., Zecchina, A., and Bellussi, G., *J. Phys. Chem.* **101**, 4740 (1997).
43. Hunger, H., Horvath, T., and Weitkamp, J., *Microporous Mesoporous Mater.* **22**, 357 (1998).